

# Encapsulation of *Trichoderma harzianum* with nanocellulose/carboxymethyl cellulose nanocomposite

Mariana Brondi<sup>a,b</sup>, Camila Florencio<sup>a</sup>, Luiz Mattoso<sup>a</sup>, Caue Ribeiro<sup>a</sup>, Cristiane Farinas<sup>a,b,\*</sup>

<sup>a</sup> Embrapa Instrumentation, Rua XV de Novembro 1452, 13560-970 São Carlos, SP, Brazil

<sup>b</sup> Graduate Program of Chemical Engineering, Federal University of São Carlos, 13565-905 Sao Carlos, SP, Brazil

## ARTICLE INFO

### Keywords:

Cellulose nanocrystals  
Carboxymethyl cellulose  
Microbial inoculant  
Encapsulation

## ABSTRACT

This study proposes the use of green matrices of cellulose nanocrystals (CNC) and a nanocomposite of CNC with carboxymethyl cellulose (CMC) for efficiently encapsulating the plant biocontrol agent *Trichoderma harzianum*. Beads containing spores of the microorganism were produced by dripping dispersions of the polymers into a CaCl<sub>2</sub> coagulation bath, resulting in the crosslinking of CNC chains by Ca<sup>2+</sup> ions. SEM micrographs evidenced the *T. harzianum* spores in the encapsulation matrices. X-ray microtomography confirmed the random distribution of the microorganism within the polymeric matrix and the presence of internal pores in the CNC:CMC:spores beads. Encapsulation in the CNC:CMC nanocomposite favored growth of the fungus after 10 days of storage at room temperature, which could be attributed to the presence of internal pores and to the extra carbon source provided by the CMC. The results indicated that CNC:CMC nanocomposites are promising materials for protecting and delivering microbial inoculants for agricultural applications.

## 1. Introduction

Increased crop productivity is crucial for meeting the growing global demand for food. Chemical fertilizers and pesticides are essential tools for enhancing agricultural production, but the uncontrolled use of these products can negatively affect the environment. Therefore, the challenge is to identify and develop more sustainable practices, such as biofertilization employing materials inoculated with beneficial microorganisms (Sammauria et al., 2020; Santos et al., 2019). These bio-based products contain living microorganisms that can increase nutrient availability and plant growth, act as biocontrol agents against phytopathogens, mitigate the effects of stressful conditions (such as salt, drought, pH, and temperature), and/or release biostimulants and phytohormones (Egamberdieva et al., 2017; Kour et al., 2020; Seenivasagan & Babalola, 2021). Among the microbial inoculants, the fungus *Trichoderma harzianum* has been widely reported as a biocontrol agent for important crops including soybean, wheat, and maize (Mona et al., 2017; Saravanakumar et al., 2017; Zhang et al., 2016). For instance, its inoculation on soybean plants decreased the effect of the phytopathogen *Sclerotinia sclerotiorum* by 56 % (Zhang et al., 2016). *T. harzianum* can also act to increase nutrient solubilization and uptake by plants, as well as the release of phytohormones, enhancing the resistance of plants to

stressful conditions (Ghorbanpour et al., 2018; Mona et al., 2017; Ye et al., 2020).

The shelf-life of these bio-based products remains a challenge that can hinder their applications, with the inoculant formulation being of paramount importance. A suitable carrier should maintain the microorganism viable from the time of manufacture of the product until its targeted use (Kaminsky et al., 2019; Qiu et al., 2019). The encapsulation of microbial inoculants can provide a suitable medium for microorganism delivery, protecting against weathering and other stresses, and ideally ensuring conditions for adaptation of the organism after application on crops (Schoebitz et al., 2013; Vassilev et al., 2020). Natural polysaccharides such as alginate, chitosan, and starch have the advantage of biodegradability (Vassilev et al., 2020). For instance, the use of alginate-based matrices for encapsulation can improve the microorganism protection against some abiotic stresses, increasing the shelf-life (Locatelli et al., 2018; Maruyama et al., 2020). However, these biopolymers matrices usually present a unstable capsule structure or limited loading capacity (Vassilev et al., 2020). One way to address these problems is to use compositions with nanoparticles, such as nanocomposites (Kumar et al., 2021). For example, the use of nanocellulose-reinforced polymers can maintain complete biodegradability and improve the mechanical properties of the formulation,

\* Corresponding author at: Embrapa Instrumentation, Rua XV de Novembro 1452, 13560-970 São Carlos, SP, Brazil.

E-mail address: [cristiane.farinas@embrapa.br](mailto:cristiane.farinas@embrapa.br) (C. Farinas).

<https://doi.org/10.1016/j.carbpol.2022.119876>

Received 2 May 2022; Received in revised form 1 July 2022; Accepted 12 July 2022

Available online 19 July 2022

0144-8617/© 2022 Elsevier Ltd. All rights reserved.

enabling a wide range of applications (Nascimento et al., 2018).

Carboxymethyl cellulose (CMC) has emerged as an ideal matrix for these nanocomposites, given its natural compatibility with nanocellulose structures (Oun & Rhim, 2017). Both cellulose nanocrystals (CNC) and CMC can be easily used to prepare capsules by different techniques (Calegari et al., 2022; Fitri et al., 2022; Levin et al., 2018; Nie et al., 2021). Therefore, the present work proposes the use of nanocellulose:CMC nanocomposite (CNC:CMC) as a system suitable for protecting *T. harzianum*, employed as a model microorganism. The results showed that the nanocomposite capsules could be prepared by a simple coagulation route, according to a straightforward dripping method. Following the encapsulation process, the protected *T. harzianum* was capable of growth after 10 days of dry storage at room temperature. The procedure could be extended to other microorganisms, making CNC:CMC a versatile and sustainable platform for the delivery of agriculturally relevant microorganisms.

## 2. Materials and methods

### 2.1. Materials

Cellulose nanocrystals (CNCs) (Celluforce, Canada) and sodium carboxymethyl cellulose (CMC - medium viscosity and with a degree of substitution of 0.7) (Synth, Brazil) were used as the encapsulation matrices. The CNCs were obtained by hydrolysis with sulfuric acid (64 wt%), leading to the addition of sulfate half-ester groups at the surface (Reid et al., 2017). According to the manufacturer, it has an average nominal diameter of 7.5 nm and a length of 150 nm, with an aspect ratio of 20. Calcium chloride ( $\text{CaCl}_2$ ) (Synth, Brazil) was used as the cross-linking agent. Tween 80 (Dinâmica, Brazil) was employed to extract the spores of the filamentous fungus. All the materials were used as received. The *Trichoderma harzianum* LQC-99 strain was provided by Embrapa Environment (Brazil).

### 2.2. *Trichoderma harzianum* cultivation and spore extraction

*Trichoderma harzianum* LQC-99 was used as a model microorganism to evaluate the effects of encapsulation in CNC and CNC:CMC on a well-known microbial inoculant (Fraceto et al., 2018; Maruyama et al., 2020). The spores were germinated at 28 °C in Petri dishes containing potato dextrose agar (PDA). After 7 days, a 1 % (w/v) Tween 80 solution was used to collect the spores, which were then concentrated by centrifugation for 10 min at 8000 rpm. The spore concentration was determined using a Neubauer chamber.

### 2.3. Beads preparation

A preliminary evaluation (reported in the Supplementary material) was used to define the CNC, CMC, and  $\text{CaCl}_2$  concentrations employed. Nanocomposite beads were produced by coagulation. For the reference samples without spores (Fig. 1a), CNC and CMC were dispersed in distilled water and stirred overnight, with final concentrations of 5 % (w/v) and 1.5 % (w/v), respectively. Dispersions of pure CNC and a CNC:CMC mixture (3:1 by volume) were evaluated as the primary materials of the encapsulation matrices. The process was carried out by dripping the polymeric dispersions into a 1 M  $\text{CaCl}_2$  coagulation bath, at room temperature, using a 3 mL syringe and a needle.  $\text{CaCl}_2$  is widely used as a crosslinking agent in the production of alginate beads (Lan et al., 2018). The  $\text{Ca}^{2+}$  ions can form ionic interactions between the negatively charged groups of cellulose (and its derivatives) and nanocellulose molecules (after previous functionalization of the polymers to induce charges), resulting in the formation of beads when the polymeric dispersion is dripped into  $\text{CaCl}_2$  solution (de Carvalho et al., 2016; Ferrari et al., 2021). The beads formed were kept in the salt solution for 30 min, washed with distilled water to remove the excess salt, and then dried in an oven at 28 °C for 48 h. Additionally, some of the beads were

lyophilized to remove residual water, prior to characterization using FTIR, TGA, and DSC techniques.

For the encapsulation of the microorganism (Fig. 1b), all dispersions were previously autoclaved at 121 °C for 15 min, and the procedure was performed under sterile conditions in a laminar flow of air. A concentration of  $10^9$  spores/g was added to the CNC and CNC:CMC dispersions, with stirring for 15 min and then dripping into 1 M  $\text{CaCl}_2$  solution. The beads were kept in the bath for 30 min, followed by washing with distilled water and storing in water in a refrigerator (at 4 °C). Some of the beads were also dried in an oven at 28 °C for 48 h and subsequently stored at room temperature. The encapsulation efficiency was determined using the Neubauer chamber to quantify the spores remaining in the  $\text{CaCl}_2$  solution after the coagulation process.

### 2.4. Films preparation

The thermal and chemical characteristics of the CNC, CMC, and CNC:CMC materials were investigated by preparing films after dispersion of the samples in water at concentrations of 5 % (w/v) CNC, 1.5 % (w/v) CMC, and CNC:CMC composite at a volume ratio of 3:1 (CNC dispersion: CMC dispersion). These solutions were stirred overnight until complete dispersion. For the contact angle measurements, *T. harzianum* spores were added to the dispersions at a concentration of  $10^9$  spores/g of material, under stirring for 15 min. The dispersions were then spread on Teflon plates and oven-dried for 48 h at 28 °C.

### 2.5. Characterizations

Morphological evaluation of the CNC and CNC:CMC beads with and without the microorganism spores was performed using an optical stereomicroscope (Stemi 2000-C, Zeiss) and a scanning electron microscope (SEM) (JSM-6510, JEOL). X-ray microtomography (Model 1172, SkyScan) was used to evaluate the internal structures of the bead matrices and the dispersions of CNC, CMC, and spores. Static water contact angle measurements (CAM 101, KVS Instruments) were performed to evaluate the interactions of the CNC and CNC:CMC films with water, and to determine the effect of spore addition on the hydrophilic properties of the films.

The thermal and chemical characterization of the beads and films (without the spores) was performed by thermogravimetric analyses (TGA – Q500 analyzer, TA Instruments), differential scanning calorimetry (DSC - Q100 analyzer, TA Instruments) and Fourier transform infrared spectroscopy (FTIR - Vertex 70 instrument (Bruker) equipped with an attenuated total reflectance (ATR) accessory). A detailed description of the characterization techniques is presented in Supplementary material.

### 2.6. Effect of encapsulation on microorganism growth

The effect of encapsulation on the growth of the microorganism was assessed 10 days after the coagulation process. The beads (CNC and CNC:CMC matrices) containing the encapsulated microorganism, which had been kept in a refrigerator (wet) with temperature between 2 and 6 °C or at room temperature (dry) with temperature around 25 °C, were placed in the centers of Petri dishes containing potato dextrose agar (PDA). The PDA solution was prepared according to the manufacturer (Acumedia, USA). After microorganisms' inoculation, the plates were kept in a Bio-Oxygen demand (BOD) incubator at 28 °C for 10 days. The development of the fungus was then followed by imaging analysis, using ImageJ software. For comparison, the solution of free spores that had been stored under refrigeration was also evaluated, using the same spore concentration as for the encapsulated spores.

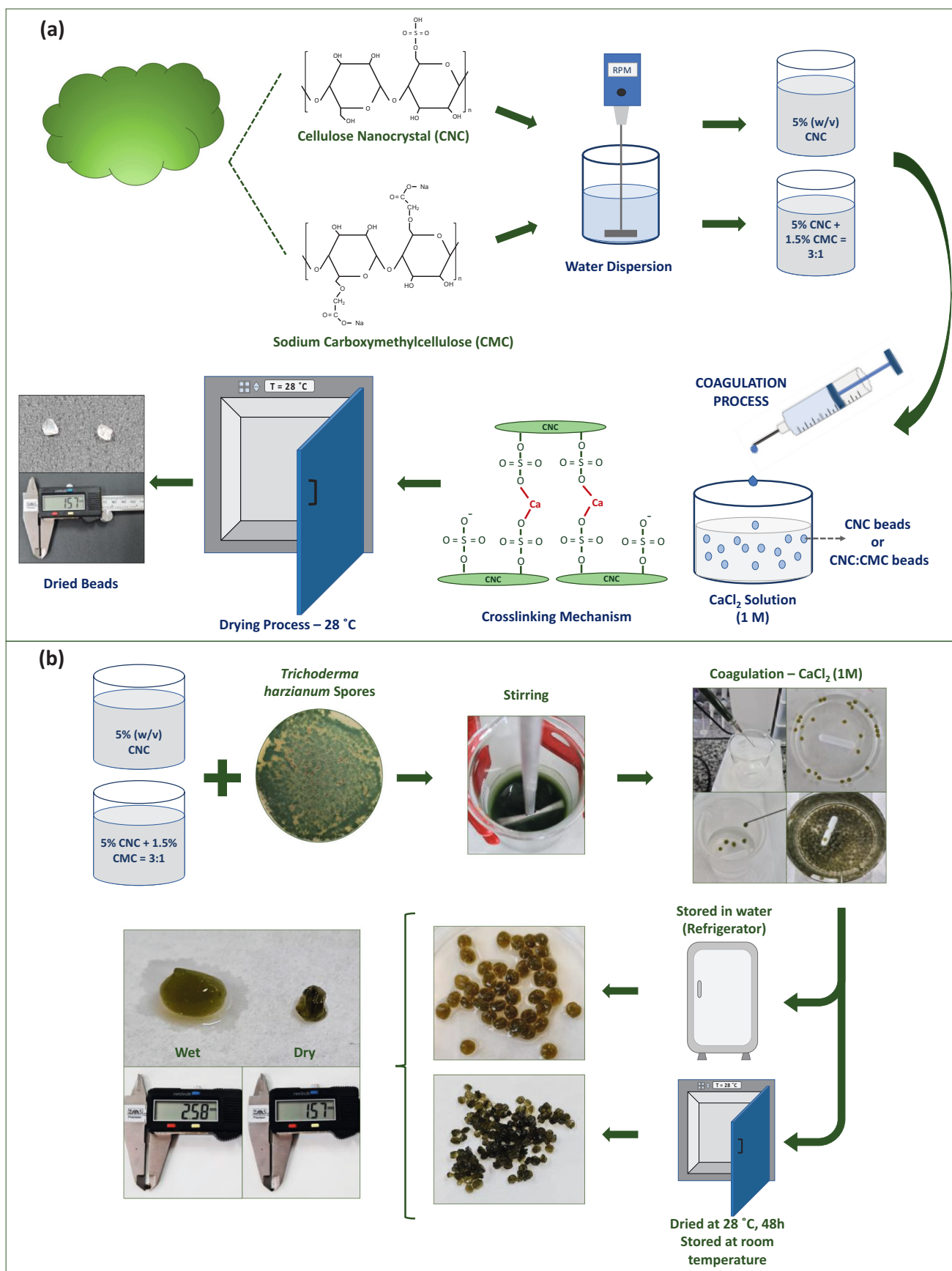


Fig. 1. Schematic representation of production of the beads: (a) without the microorganism and (b) with the *Trichoderma harzianum* spores ( $10^9$  spores/g).

### 3. Results and discussion

#### 3.1. Preparation and morphological characterization of the beads

Fig. 1a shows the coagulation of the beads without *T. harzianum* and a schematic representation of the crosslinking mechanism, while Fig. 1b shows the process with encapsulation of the fungus. The spore encapsulation efficiency was  $99.98 \pm 0.01$  %. It can be seen from Fig. 1a and b that the presence of *T. harzianum* in the matrix did not influence the size of the spheres. The average diameter of the wet beads was  $2.58 \pm 0.12$  mm, while the dried beads presented a lower average value of  $1.57 \pm 0.19$  mm (Fig. 1b), due to moisture loss. The drying step was considered essential, since it could mitigate the effect of high temperature on cell viability (Fraceto et al., 2018; Su et al., 2008). It is believed that performing the encapsulation process at lower temperatures results in less inhibition of the growth of microorganisms, including fungi of the genus *Trichoderma*, for which the best growth occurs at temperatures close to 30 °C. Therefore, in addition to the thermal and chemical characterizations of the beads, experiments were carried out to observe the growth of the microorganism in the presence of the different polymers.

Morphological characterizations of the beads of pure CNC and the CNC:CMC nanocomposite, in the presence and absence of *T. harzianum* spores, were performed by stereomicroscopy (Fig. 2a and b) and SEM (Fig. 2c–e). The pure CNC beads presented a rougher surface, which could have resulted from the oven-drying process (at 28 °C for 48 h) and stronger ionic crosslinking interactions, while the surfaces of the CNC:CMC beads were less irregular. The CNC and CNC:CMC beads both exhibited a dense and compact microstructure, with some cracks on their surfaces. There was no evidence of agglomeration of the polymers (within the detection limits of the equipment), indicating good miscibility of CMC in the CNC matrix. Neither matrices (without the spores) showed a porous structure, which could be a result of the ionic interactions (crosslinking) between the  $\text{Ca}^{2+}$  ions and the CNC, resulting in a denser structure (Huq et al., 2017; Nie et al., 2021).

The spheres were fractured by immersion in liquid nitrogen, in order to be able to visualize the microorganisms inside the matrix structure by

SEM analysis. The *T. harzianum* spores present within the capsules can be seen (green color) in Fig. 2d and e. The average spore diameter calculated using ImageJ software was  $2.14 \pm 0.22$   $\mu\text{m}$ , which was in agreement with the average size reported by Muñoz-Celaya et al. (2012). The green color of the beads with the encapsulated microorganism resulted from addition of the *T. harzianum* spores (Fig. 1b).

#### 3.2. X-ray microtomography and contact angle analyses

The X-ray microtomography results (Fig. 3) showed no evidence of agglomeration, indicating good dispersion of the components in the encapsulation matrix. Considering pores and cracks, all the beads presented a dense structure (within the detection limits of the equipment), with the exception of the CNC:CMC:*T. harzianum* beads, for which the structure was probably influenced by air bubbles trapped inside the matrix after the coagulation process. The addition of the concentrated spores solution, followed by the mixing process, resulted in the entrapment of some air bubbles within the encapsulation matrix, due to the high viscosity of the CNC:CMC dispersion (see the video provided as Supplementary material).

The contact angle analysis indicated the interactions between the materials and water. Sodium CMC is water-soluble (Guo et al., 2019), while cellulose nanocrystals usually have strong affinity for water, although they do not dissolve in water (Vanderfleet & Cranston, 2021). As shown in Fig. 3, the CNC and CNC:CMC films both presented a contact angle smaller than 90° (66.8° and 57.7°, respectively), reflecting hydrophilic behavior. The smaller angles for the nanocomposite (CNC:CMC) could be explained by the addition of CMC, which has higher water affinity, compared to CNC (Mandal & Chakrabarty, 2019). The presence of spores did not change the wettability of the CNC:CMC film. However, for the CNC film, the addition of the spores caused the contact angle to decrease from 66.8° to 45.1°. In all cases, the contact angles decreased after 60 s of interaction, especially for the nanocomposite film (with and without spores) and the CNC film with spores. Although the CNC and CNC:CMC films were hydrophilic, it is important to highlight that they presented higher water contact angles than obtained for

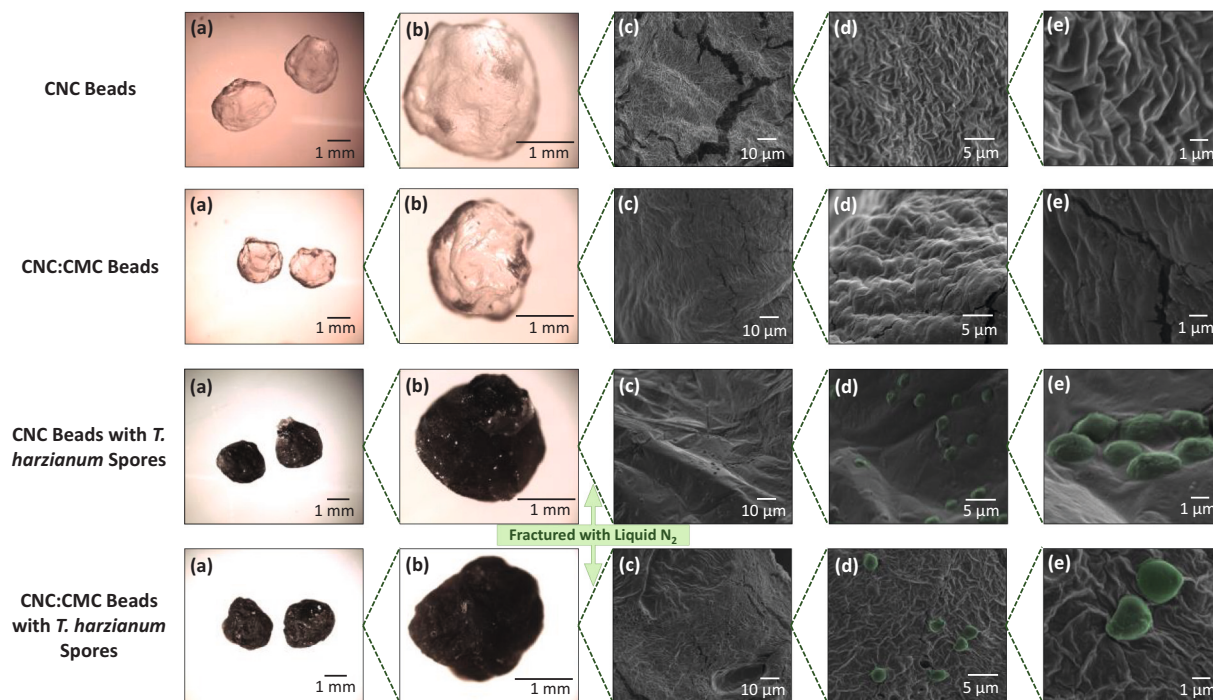
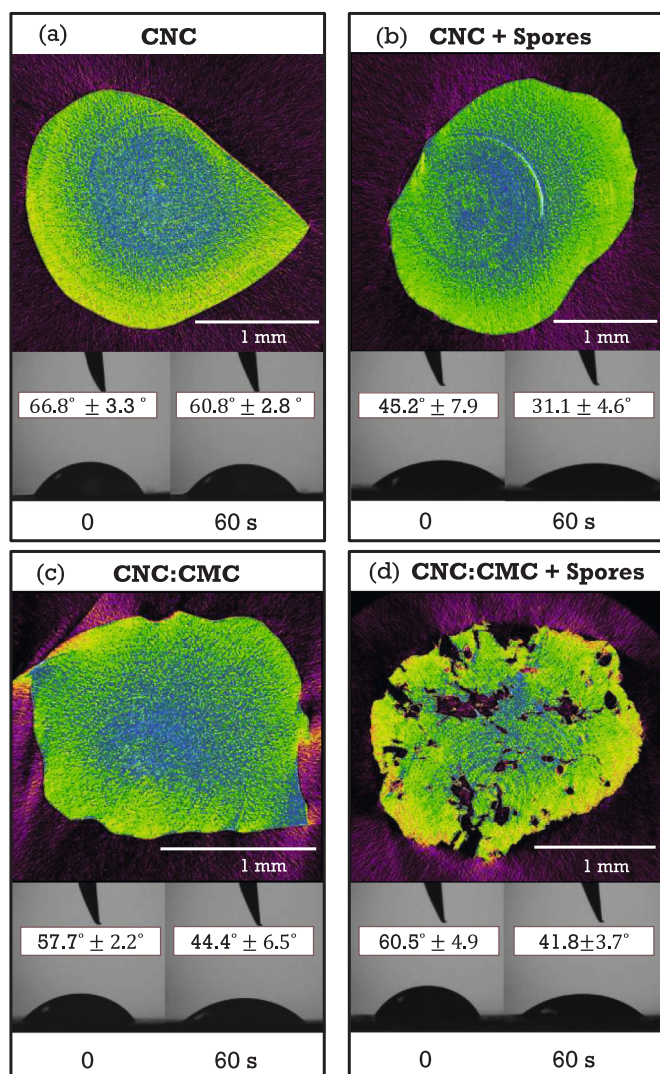


Fig. 2. Stereomicroscopy photomicrographs (a, b) and SEM micrographs (c–e), obtained at different magnifications, of the CNC and CNC:CMC nanocomposite beads with and without *Trichoderma harzianum*. The spores were colored green by the GIMP 2.10 software. (For interpretation of the references to color in this figure legend, the reader is referred to the web version of this article.)



**Fig. 3.** X-ray microtomography images of the beads and water contact angles of the films, in the presence and absence of the microorganism spores: (a) CNC, (b) CNC:*T. harzianum*, (c) CNC:CMC, and (d) CNC:CMC:*T. harzianum*.

alginate, the material most widely used for the encapsulation of microbial inoculants (Holler et al., 2018; Lavrić et al., 2021). This property could be attractive for agricultural applications, enabling slower and controlled release of the microorganism after application to crops (Campos et al., 2014; Vassilev et al., 2020).

### 3.3. Thermal and chemical characterizations

The results of the TGA and DTG thermal decomposition analyses of the samples are shown in Fig. 4a and b, respectively. All the films showed slight water evaporation at around 50–120 °C. The onset of thermal degradation of the CNC and CNC:CMC films occurred at ~215 °C. The TGA curves showed mass losses in the first thermal degradation event of approximately 30 % for the CNC film (at 215–275 °C) and 5 % for the CNC:CMC film (at 215–235 °C). These results reflected slower degradation of the composite, compared to the pure CNC, which could be explained by the existence of hydrogen bonds between CNC and CMC (pseudo-crosslinks between the polymers) (Mandal & Chakrabarty, 2019). In the temperature range 275–450 °C, the CNC film showed 25 % mass loss, compared to a value of approximately 50 % for the CNC:CMC film. Thermal degradation of the CMC film started at ~250 °C, with mass loss of around 20 % up to the

maximum temperature of 500 °C used in the TGA measurements. The lower degradation temperature of CNC obtained by sulfuric acid hydrolysis, compared to CMC, has been reported previously (Choi & Simonsen, 2006; Li, Shi, et al., 2020). The higher surface area of CNC could act to increase the exposure to heat, consequently reducing the thermal stability (Hu et al., 2014). It has also been suggested that the concentration of the sulfuric acid used in the production of CNC influences the thermal degradation behavior of the resulting material (Gong et al., 2017).

The thermal degradation profiles of the CNC and CNC:CMC beads were similar. In both cases, a water evaporation event occurred between 50 and 120 °C, with mass losses of ~28 % and ~21 % for CNC and CNC:CMC, respectively. These higher water contents of the beads obtained using the crosslinking process with CaCl<sub>2</sub> could have been due to the entrapment of water within the bead structures. Furthermore, since CaCl<sub>2</sub> is a hygroscopic salt, its residues remaining in the beads could have acted to increase the water content. The onset temperature for thermal degradation of the beads (~175 °C) was lower than for the films. From 175 to 300 °C, the CNC beads presented a mass loss of 17 %, while the CNC:CMC composite beads lost ~22 %. Previous studies have also reported decreases in the thermal degradation onset temperatures of composites, compared to pure polymers, due to the effect of Ca<sup>2+</sup> ionic crosslinking (Abitbol et al., 2021; Kumar et al., 2017; Uyanga & Daoud, 2021).

Fig. 4c shows the DSC results for the films and beads. The endothermic peaks in DSC curves, in the temperature range 50–150 °C, are usually related to heat adsorption as water evaporates from the materials (Asma et al., 2014; Lima et al., 2020). The DSC curve for the CNC film showed a shallow endothermic event. Although the hydroxyl groups on CNC attract water molecules, the presence of sulfate groups reduces the hygroscopicity of this material, leading to a smaller energy demand to evaporate water (Li, Shi, et al., 2020). In the case of CMC, the presence of hydroxyl and carboxylate groups increases the affinity for moisture absorption, leading to an increase in the width of the endothermic peak corresponding to water evaporation (Mandal & Chakrabarty, 2019). The curve for the CNC:CMC composite (Fig. 4c) showed an intermediate behavior of the endothermic peak.

The behaviors of the DSC curves for the CNC and CNC:CMC beads were similar, with the ionic crosslinking process resulting in increased endothermic peak widths and temperatures for water evaporation. The CNC:CMC composite beads required higher energy absorption for water evaporation, compared to the pure CNC beads, due to the higher water affinity of CMC. Another endothermic event was observed at 180–210 °C, for both types of beads. As found in the TGA analysis, these peaks were related to the thermal degradation of the materials. The main events observed by the TGA and DSC analyses are described in the Supplementary material (Table S2).

Fig. 4d shows the FTIR spectra of the films formed by dispersing the materials (CNC, CNC:CMC, and CMC) in water and then oven-drying, together with the spectra for the lyophilized CNC and CNC:CMC beads. The spectra reflected the similar chemical structures of CNC and CMC. The spectra for the beads obtained after the crosslinking process showed an increase of the band at 3335 cm<sup>-1</sup> (ascribed to stretching of the -OH groups present in both CNC and CMC), compared to the spectra for the films. This could be explained by the Ca<sup>2+</sup> crosslinking process, with formation of stronger hydrogen bonds between the CNC and CNC:CMC chains (Mandal & Chakrabarty, 2019; Nie et al., 2021). The intensity of the -OH band was lower for CMC, because some of the -OH groups had been substituted by -CH<sub>2</sub>COONa during the production process (Alizadeh Asl et al., 2017). Bands at 2900 and 1630 cm<sup>-1</sup> were related to C—H stretching and -OH bending vibrations, respectively. The CMC spectrum presented a peak at 1587 cm<sup>-1</sup>, attributed to the -COO<sup>-</sup> group, which was not observed in the spectra for the other matrices (or was very small for CNC:CMC, due to the low CMC content). This peak was related to the carboxymethyl groups present at the CMC surface. Bands at around 1427 cm<sup>-1</sup> (1412 cm<sup>-1</sup> for CMC), 1371 cm<sup>-1</sup>, and

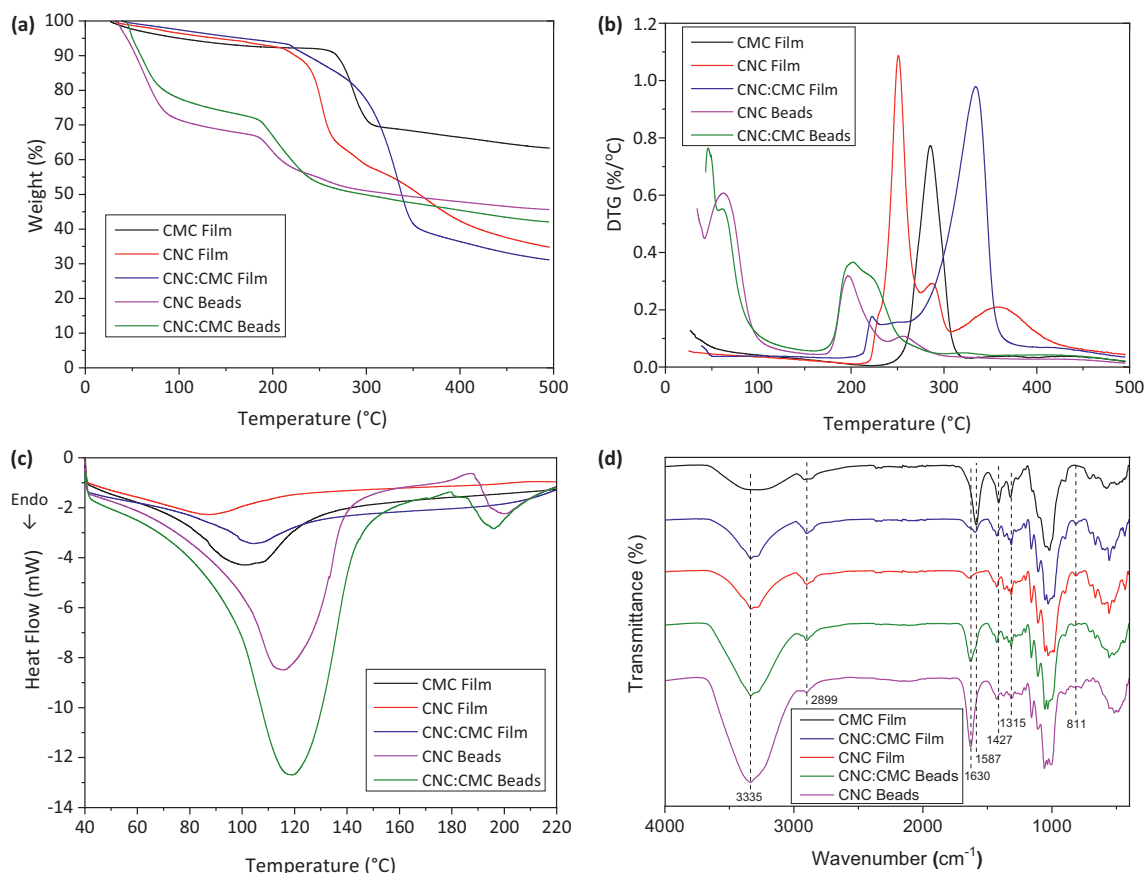


**Fig. 4.** Thermal and chemical characterizations of CNC, CMC, a mixture of CNC and CMC (3:1 ratio), and the lyophilized CNC and CNC:CMC beads: (a) thermogravimetric analysis (TGA), (b) derivative thermogravimetry (DTG), (c) differential scanning calorimetry (DSC), and (d) Fourier transform infrared spectroscopy (FTIR).

$1315\text{ cm}^{-1}$  were assigned to  $-\text{CH}_2-$  symmetric bending and the bending vibrations of C—H and C—O groups at the ring, respectively (Kusmono et al., 2020; Mandal & Chakrabarty, 2019). Peaks in the range  $1000\text{--}1200\text{ cm}^{-1}$  were attributed to ether group  $-\text{O}-$  stretching (Alizadeh Asl et al., 2017). A small peak at  $811\text{ cm}^{-1}$ , observed in the spectra for all the samples with CNC, was related to the C-O-S group of sulfate ester, which was present on the surface due to the use of sulfuric acid hydrolysis in CNC production (Jasmani & Adnan, 2017; Kusmono et al., 2020).

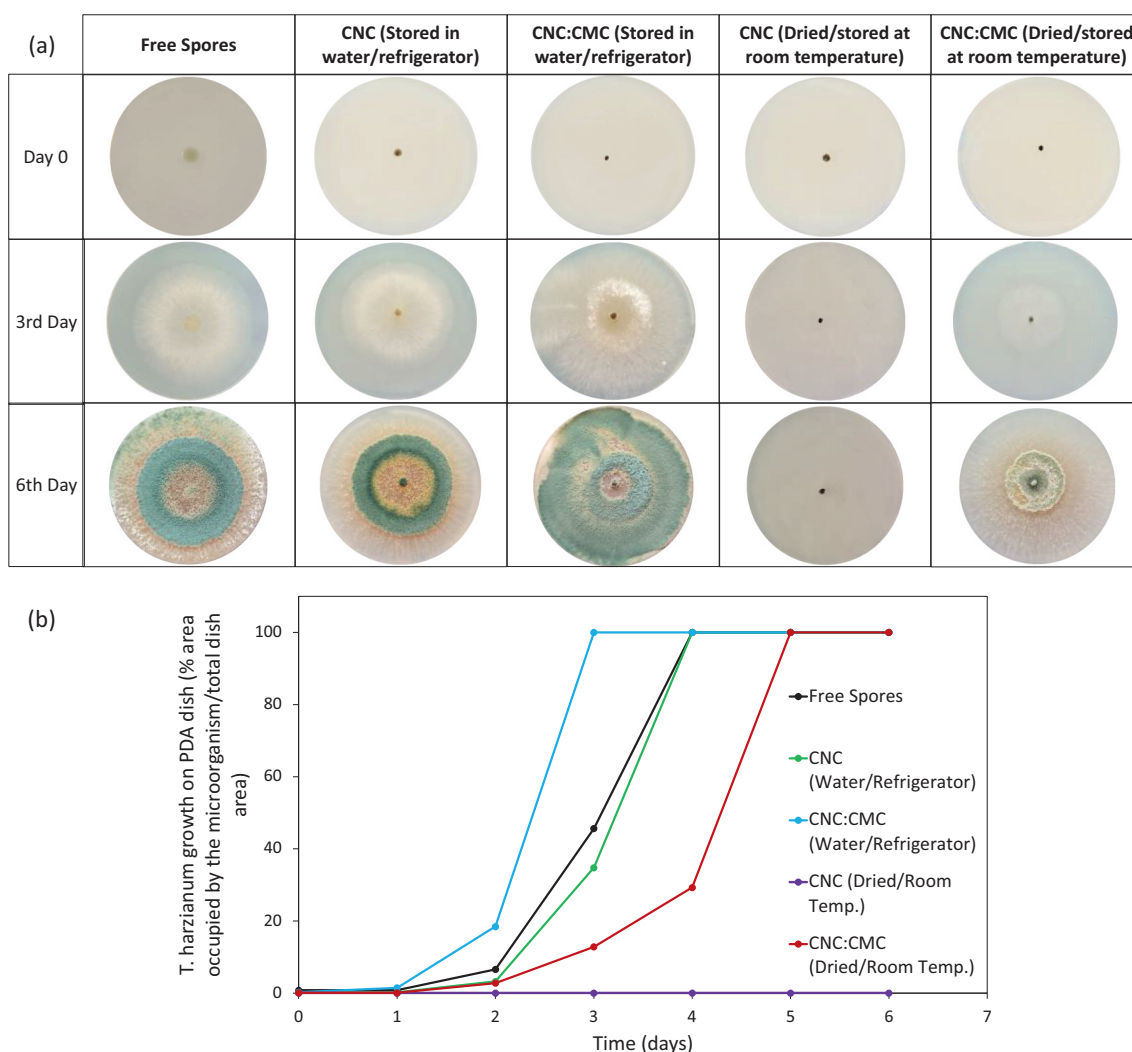
### 3.4. Effect of encapsulation on microorganism growth

Fig. 5a shows the effect of encapsulation on growth of the fungus in the Petri dishes containing PDA, observed 10 days after the encapsulation process. The CNC and CNC:CMC beads containing the microorganism spores were previously stored wet (under refrigeration) and dried (at room temperature). The growth of the encapsulated microorganism was compared to that of the free spores in solution, stored under refrigeration. For most of the conditions, with the exception of the dried CNC beads, the fungus was able to grow on the PDA, but at different growth rates. The fastest rate was observed for the refrigerated (wet) CNC:CMC beads (Fig. 5b), where the CMC present in the matrix provided an additional source of carbon for the microorganism (Bashan et al., 2014; Gelain et al., 2021). *T. harzianum* has been found to produce cellulases capable of degrading cellulosic substrates after 24 h of cultivation (da Silva Delabona et al., 2016; Li, Zhang, et al., 2020). Therefore, the release of these enzymes could assist the microorganism in degrading the CNC:CMC matrix, enhancing its growth in the PDA medium. In addition, as shown by the X-ray microtomography results

(Fig. 3), the internal pores in the beads could act to increase diffusion of the spores from the beads to the PDA.

The growth rate observed for the refrigerated (wet) beads was similar to, or better than, that for the free spores. Possible explanations were the extra protection that encapsulation provided against stress occurring during the storage period, as well as the additional carbon source present in the encapsulation matrix (Chanratana et al., 2018; He et al., 2015; Vassilev et al., 2020). It is also important to point out that the viability of the microorganism was affected by the storage temperature and the drying process (Chanratana et al., 2018; He et al., 2015), since the fungus present in the refrigerated (wet) CNC beads was able to occupy the entire dish after 4 days, while the fungus in the dried CNC beads was unable to grow. It is also possible that the lower growth rate observed for the pure CNC beads, compared to the CNC:CMC composite, could have been influenced by damage to the cell membranes of the microorganism by the sharp edges of the CNC, causing cell inactivation (Noronha et al., 2021). The addition of CMC to the encapsulation matrix may have provided protection against this effect.

Comparison of the dried/room temperature CNC:CMC with the refrigerated/wet CNC:CMC nanocomposite showed that the latter presented faster growth. The drying process and the storage at room temperature could have decreased the viability of the fungus, because the spores had greater exposure to environmental factors such as temperature and humidity changes. However, it was expected that encapsulation would provide the cells with protection against these conditions. The lower water content within the matrix of the dried beads would lead to slower metabolic activity of the microorganisms, consequently decreasing the growth rate (which could assist in increasing the shelf-life of the product) (Santos et al., 2019), as well as reduce diffusion of the



**Fig. 5.** (a) Growth in PDA medium of the free spores and the spores encapsulated in the CNC and CNC:CMC (3:1) beads previously stored for 10 days under wet/refrigerated or dry/room temperature conditions, evaluated by photographs obtained during 6 days. (b) Percentages of the Petri dish areas occupied by *Trichoderma harzianum*, determined using ImageJ software.

cells from the bead matrix to the PDA medium. The compact structure of the dried beads, shown in the SEM micrographs (Fig. 2), could also have contributed to reducing diffusion of the cells. These attractive characteristics would ensure the desired slow release of the microorganism, following application of the product to crops.

#### 4. Conclusions

Beads composed of CNC and CNC:CMC nanocomposite were produced by ionic crosslinking using  $\text{Ca}^{2+}$  ions and were effectively employed for microbial encapsulation. Determination of the growth rates of the free and encapsulated microorganisms in PDA medium showed that the growth was influenced by the drying process and the storage temperature. The addition of CMC to the CNC matrix was essential for the growth of *T. harzianum* after storage under dry conditions for 10 days following the encapsulation process. These results indicated that CNC:CMC beads are an attractive green matrix for the encapsulation of microorganisms used in the agricultural sector such as inoculants, biofertilizers and biocontrol agents. Benefits regarding an improved product shelf-life and protection against stress conditions are expected upon future application in the field.

Supplementary data to this article can be found online at <https://doi.org/10.1016/j.carbpol.2022.119876>.

#### CRediT authorship contribution statement

**Mariana Brondi:** Conceptualization, methodology, investigation, data analysis, writing – original draft. **Camila Florencio:** Conceptualization, methodology, writing – review and editing. **Luiz Mattoso:** Supervision, writing – review and editing. **Caue Ribeiro:** Conceptualization, methodology, supervision, writing – review and editing. **Cristiane Farinas:** Conceptualization, methodology, supervision, writing – review and editing.

#### Declaration of competing interest

The authors declare that they have no known competing financial interests or personal relationships that could have appeared to influence the work reported in this paper.

#### Data availability

Data will be made available on request.

#### Acknowledgments

The authors are grateful for financial support provided by the

following Brazilian research funding agencies: State of São Paulo Research Foundation (FAPESP, grants 2016/10636-8, 2019/25261-8 and 2019/05159-4), National Council for Scientific and Technological Development (CNPq, grant 141303/2019-0), and Coordination for the Improvement of Higher Education Personnel (CAPES, Finance Code 001). We also would like to thank Prof. Dr. Dagoberto Brandão Santos for the stereomicroscopy analyses.

## References

- Abitbol, T., Mijlkovic, A., Malafronte, L., Stevanic, J. S., Larsson, P. T., & Lopez-Sanchez, P. (2021). Cellulose nanocrystal/low methoxyl pectin gels produced by internal ionotropic gelation. *Carbohydrate Polymers*, *260*, Article 117345. <https://doi.org/10.1016/j.carbpol.2020.117345>
- Alizadeh Asl, S., Mousavi, M., & Labbafi, M. (2017). Synthesis and characterization of carboxymethyl cellulose from sugarcane bagasse. *Journal of Food Processing & Technology*, *08*. <https://doi.org/10.4172/2157-7110.1000687>
- Asma, C., Meriem, E., Mahmoud, B., & Djafer, B. (2014). Physicochemical characterization of gelatin-CMC composite edibles films from polyion-complex hydrogels. *Journal of the Chilean Chemical Society*, *59*, 2279–2283. <https://doi.org/10.4067/S0717-97072014000100008>
- Bashan, Y., de Bashan, L. E., Prabhu, S. R., & Hernandez, J. P. (2014). Advances in plant growth-promoting bacterial inoculant technology: Formulations and practical perspectives (1998–2013). *Plant Soil*, *378*, 1–33. <https://doi.org/10.1007/s11104-013-1956-x>
- Calegari, F., Sousa, I., Ferreira, M. G. S., Berton, M. A. C., Marino, C. E. B., & Tedim, J. (2022). Influence of the operating conditions on the release of corrosion inhibitors from spray-dried carboxymethylcellulose microspheres. *Applied Sciences*, *12*, 1800. <https://doi.org/10.3390/app12041800>
- Campos, E. V. R., de Oliveira, J. L., Fraceto, L. F., & Singh, B. (2014). Polysaccharides as safer release systems for agrochemicals. *Agronomy for Sustainable Development*, *35*, 47–66. <https://doi.org/10.1007/s13593-014-0263-0>
- Chanratana, M., Han, G. H., Melvin Joe, M., Roy Choudhury, A., Sundaram, S., Halim, M. A., & Sa, T. (2018). Evaluation of chitosan and alginate immobilized methylbacterium oryzae CBMB20 on tomato plant growth. *Archives of Agronomy and Soil Science*. <https://doi.org/10.1080/03650340.2018.1440390>
- Choi, Y., & Simonsen, J. (2006). Cellulose nanocrystal-filled carboxymethyl cellulose nanocomposites. *Journal of Nanoscience and Nanotechnology*, *6*, 633–639. <https://doi.org/10.1116/jnn.2006.132>
- da Silva Delabona, P., Lima, D. J., Robl, D., Rabelo, S. C., Farinas, C. S., & da Cruz Pradella, J. G. (2016). Enhanced cellulase production by trichoderma harzianum by cultivation on glycerol followed by induction on cellulosic substrates. *Journal of Industrial Microbiology & Biotechnology*, *43*, 617–626. <https://doi.org/10.1007/s10295-016-1744-8>
- de Carvalho, R. A., Veronese, G., Carvalho, A. J. F., Barbu, E., Amaral, A. C., & Trovatti, E. (2016). The potential of TEMPO-oxidized nanofibrillar cellulose beads for cell delivery applications. *Cellulose*, *23*, 3399–3405. <https://doi.org/10.1007/s10570-016-1063-2>
- Egamberdieva, D., Wirth, S. J., Alqarawi, A. A., Abd-Allah, E. F., & Hashem, A. (2017). Phytohormones and beneficial microbes: essential components for plants to balance stress and fitness. *Front. Microbiol.*, *8*. <https://doi.org/10.3389/fmicb.2017.02104>
- Ferrari, N., Maestri, C. A., Bettotti, P., Grassi, M., Abrami, M., & Scarpa, M. (2021). Effect of process conditions and colloidal properties of cellulose nanocrystals suspensions on the production of hydrogel beads. *Molecules*, *26*, 2552. <https://doi.org/10.3390/molecules26092552>
- Fitri, I. A., Mitbunrung, W., Akanitkul, P., Rungraeng, N., Kemsawasud, V., Jain, S., & Winuprasith, T. (2022). Encapsulation of β-carotene in oil-in-water emulsions containing nanocellulose: Impact on emulsion properties, in vitro digestion, and bioaccessibility. *Polymers (Basel)*, *14*, 1414. <https://doi.org/10.3390/polym14071414>
- Fraceto, L. F., Maruyama, C. R., Guilger, M., Mishra, S., Keswani, C., Singh, H. B., & de Lima, R. (2018). Trichoderma harzianum -based novel formulations: Potential applications for management of next-gen agricultural challenges. *Journal of Chemical Technology and Biotechnology*, *93*, 2056–2063. <https://doi.org/10.1002/jctb.5613>
- Gelain, L., Kingma, E., da Cruz, G., Pradella, J., Carvalho da Costa, A., van der Wielen, L., & van Gulik, W. M. (2021). Continuous production of enzymes under carbon-limited conditions by trichoderma harzianum P49P11. *Fungal Biology*, *125*, 177–183. <https://doi.org/10.1016/j.funbio.2020.10.008>
- Ghorbanpour, A., Salimi, A., Ghanbary, M. A. T., Pirdashti, H., & Dehestani, A. (2018). The effect of Trichoderma harzianum in mitigating low temperature stress in tomato (*Solanum lycopersicum* L.) plants. *Scientia Horticulturae*, *230*, 134–141. <https://doi.org/10.1016/j.scienta.2017.11.028>
- Gong, J., Li, J., Xu, J., Xiang, Z., & Mo, L. (2017). Research on cellulose nanocrystals produced from cellulose sources with various polymorphs. *RSC Advances*, *7*, 33486–33493. <https://doi.org/10.1039/C7RA06222B>
- Guo, T., Gu, L., Zhang, Y., Chen, H., Jiang, B., Zhao, H., Jin, Y., & Xiao, H. (2019). Bioinspired self-assembled films of carboxymethyl cellulose–dopamine/montmorillonite. *Journal of Materials Chemistry A*, *7*, 14033–14041. <https://doi.org/10.1039/C9TA00998A>
- He, Y., Wu, Z., Tu, L., Han, Y., Zhang, G., & Li, C. (2015). Encapsulation and characterization of slow-release microbial fertilizer from the composites of bentonite and alginate. *Applied Clay Science*, *109–110*, 68–75. <https://doi.org/10.1016/j.clay.2015.02.001>
- Holler, S., Porcelli, C., Ieropoulos, I. A., & Hanczyc, M. M. (2018). Transport of live cells under sterile conditions using a chemotactic droplet. *Scientific Reports*, *8*, 8408. <https://doi.org/10.1038/s41598-018-26703-y>
- Hu, Y., Tang, L., Lu, Q., Wang, S., Chen, X., & Huang, B. (2014). Preparation of cellulose nanocrystals and carboxylated cellulose nanocrystals from borer powder of bamboo. *Cellulose*, *21*, 1611–1618. <https://doi.org/10.1007/s10570-014-0236-0>
- Huq, T., Frascini, C., Khan, A., Riedl, B., Bouchard, J., & Lacroix, M. (2017). Alginate based nanocomposite for microencapsulation of probiotic: Effect of cellulose nanocrystal (CNC) and lecithin. *Carbohydrate Polymers*, *168*, 61–69. <https://doi.org/10.1016/j.carbpol.2017.03.032>
- Jasmani, L., & Adnan, S. (2017). Preparation and characterization of nanocrystalline cellulose from Acacia mangium and its reinforcement potential. *Carbohydrate Polymers*, *161*, 166–171. <https://doi.org/10.1016/j.carbpol.2016.12.061>
- Kaminsky, L. M., Trexler, R. V., Malik, R. J., Hockett, K. L., & Bell, T. H. (2019). The inherent conflicts in developing slow microbial inoculants. *Trends in Biotechnology*. <https://doi.org/10.1016/j.tibtech.2018.11.011>
- Kour, D., Rana, K. L., Yadav, A. N., Yadav, N., Kumar, M., Kumar, V., Vyas, P., Dhaliwal, H. S., & Saxena, A. K. (2020). Microbial biofertilizers: Bioresources and eco-friendly technologies for agricultural and environmental sustainability. *Biocatalysis and Agricultural Biotechnology*, *23*, Article 101487. <https://doi.org/10.1016/j.bcab.2019.101487>
- Kumar, A., Choudhary, A., Kaur, H., Mehta, S., & Husen, A. (2021). Smart nanomaterial and nanocomposite with advanced agrochemical activities. *Nanoscale Research Letters*, *16*. <https://doi.org/10.1186/s11671-021-03612-0>
- Kumar, A., Lee, Y., Kim, D., Rao, K. M., Kim, J., Park, S., Haider, A., Lee, D. H., & Han, S. S. (2017). Effect of crosslinking functionality on microstructure, mechanical properties, and in vitro cytocompatibility of cellulose nanocrystals reinforced poly(vinyl alcohol)/sodium alginate hybrid scaffolds. *International Journal of Biological Macromolecules*, *95*, 962–973. <https://doi.org/10.1016/j.ijbiomac.2016.10.085>
- Kusmono, Listyanda, R. F., Wildan, M. W., & Ilman, M. N. (2020). Preparation and characterization of cellulose nanocrystal extracted from ramie fibers by sulfuric acid hydrolysis. *Heliyon*, *6*, Article e05486. <https://doi.org/10.1016/j.heliyon.2020.e05486>
- Lan, W., He, L., & Liu, Y. (2018). Preparation and properties of sodium carboxymethyl cellulose/sodium alginate/chitosan composite film. *Coatings*, *8*. <https://doi.org/10.3390/coatings8080291>
- Lavrić, G., Oberlinter, A., Filipova, I., Novak, U., Likozar, B., & Vrabčić-Brodnjak, U. (2021). Functional nanocellulose, alginate and chitosan nanocomposites designed as active film packaging materials. *Polymers (Basel)*, *13*, 2523. <https://doi.org/10.3390/polym13152523>
- Levin, D., Saem, S., Osorio, D. A., Cerf, A., Cranston, E. D., & Moran-Mirabal, J. M. (2018). Green templating of ultraporous cross-linked cellulose nanocrystal microparticles. *Chemistry of Materials*, *30*, 8040–8051. <https://doi.org/10.1021/acs.chemmater.8b03858>
- Li, H., Shi, H., He, Y., Fei, X., & Peng, L. (2020). Preparation and characterization of carboxymethyl cellulose-based composite films reinforced by cellulose nanocrystals derived from pea hull waste for food packaging applications. *International Journal of Biological Macromolecules*, *164*, 4104–4112. <https://doi.org/10.1016/j.ijbiomac.2020.09.010>
- Li, J. X., Zhang, F., Jiang, D. D., Li, J., Wang, F. L., Zhang, Z., Wang, W., & Zhao, X. Q. (2020). Diversity of cellulase-producing filamentous fungi from Tibet and transcriptomic analysis of a superior cellulase producer *Trichoderma harzianum* LZ117. *Frontiers in Microbiology*, *11*, 1–15. <https://doi.org/10.3389/fmicb.2020.01617>
- Lima, G. F., Souza, A. G., & Rosa, D. d. S. (2020). Nanocellulose as reinforcement in carboxymethylcellulose superabsorbent nanocomposite hydrogels. *Macromol. Symp.*, *394*, Article 2000126. <https://doi.org/10.1002/masy.202000126>
- Locatelli, G. O., dos Santos, G. F., Botelho, P. S., Finkler, C. L. L., & Bueno, L. A. (2018). Development of Trichoderma sp. formulations in encapsulated granules (CG) and evaluation of conidia shelf-life. *Biological Control*, *117*, 21–29. <https://doi.org/10.1016/j.biocontrol.2017.08.020>
- Mandal, A., & Chakrabarty, D. (2019). Studies on mechanical, thermal, and barrier properties of carboxymethyl cellulose film highly filled with nanocellulose. *Journal of Thermoplastic Composite Materials*, *32*, 995–1014. <https://doi.org/10.1177/0892705718772868>
- Maruyama, C. R., Bilesky-José, N., de Lima, R., & Fraceto, L. F. (2020). Encapsulation of trichoderma harzianum preserves enzymatic activity and enhances the potential for biological control. *Frontiers in Bioengineering and Biotechnology*, *8*. <https://doi.org/10.3389/fbioe.2020.00225>
- Mona, S. A., Hashem, A., Abd Allah, E. F., Alqarawi, A. A., Soliman, D. W. K., Wirth, S., & Egamberdieva, D. (2017). Increased resistance of drought by trichoderma harzianum fungal treatment correlates with increased secondary metabolites and proline content. *Journal of Integrative Agriculture*, *16*, 1751–1757. [https://doi.org/10.1016/S2095-3119\(17\)61695-2](https://doi.org/10.1016/S2095-3119(17)61695-2)
- Muñoz-Celaya, A. L., Ortiz-García, M., Vernon-Carter, E. J., Jauregui-Rincón, J., Galindo, E., & Serrano-Carreón, L. (2012). Spray-drying microencapsulation of trichoderma harzianum conidia in carbohydrate polymers matrices. *Carbohydrate Polymers*, *88*, 1141–1148. <https://doi.org/10.1016/j.carbpol.2011.12.030>
- Nascimento, D. M., Nunes, Y. L., Figueiredo, M. C. B., De Azeredo, H. M. C., Aouada, F. A., Feitosa, J. P. A., Rosa, M. F., & Dufresne, A. (2018). Nanocellulose nanocomposite hydrogels: Technological and environmental issues. *Green Chemistry*, *20*, 2428–2448. <https://doi.org/10.1039/c8gc00205c>
- Nie, G., Zang, Y., Yue, W., Wang, M., Baride, A., Sigdel, A., & Janaswamy, S. (2021). Cellulose-based hydrogel beads: Preparation and characterization. *Carbohydrate Polymer Technologies and Applications*, *2*, Article 100074. <https://doi.org/10.1016/j.carpta.2021.100074>

- Noronha, V. T., Camargos, C. H. M., Jackson, J. C., Souza Filho, A. G., Paula, A. J., Rezende, C. A., & Faria, A. F. (2021). Physical membrane-stress-mediated antimicrobial properties of cellulose nanocrystals. *ACS Sustainable Chemistry & Engineering*, 9, 3203–3212. <https://doi.org/10.1021/acssuschemeng.0c08317>
- Oun, A. A., & Rhim, J. W. (2017). Characterization of carboxymethyl cellulose-based nanocomposite films reinforced with oxidized nanocellulose isolated using ammonium persulfate method. *Carbohydrate Polymers*, 174, 484–492. <https://doi.org/10.1016/j.carbpol.2017.06.121>
- Qiu, Z., Egidi, E., Liu, H., Kaur, S., & Singh, B. K. (2019). New frontiers in agriculture productivity: Optimised microbial inoculants and in situ microbiome engineering. *Biotechnology Advances*, 37, Article 107371. <https://doi.org/10.1016/j.biotechadv.2019.03.010>
- Reid, M. S., Villalobos, M., & Cranston, E. D. (2017). Benchmarking cellulose nanocrystals: From the laboratory to industrial production. *Langmuir*, 33, 1583–1598. <https://doi.org/10.1021/acs.langmuir.6b03765>
- Sammauria, R., Kumawat, S., Kumawat, P., Singh, J., & Jatwa, T. K. (2020). Microbial inoculants: Potential tool for sustainability of agricultural production systems. *Archives of Microbiology*, 202, 677–693. <https://doi.org/10.1007/s00203-019-01795-w>
- Santos, M. S., Nogueira, M. A., & Hungria, M. (2019). Microbial inoculants: Reviewing the past, discussing the present and previewing an outstanding future for the use of beneficial bacteria in agriculture. *AMB Express*, 9. <https://doi.org/10.1186/s13568-019-0932-0>
- Saravanakumar, K., Li, Y., Yu, C., Wang, Q. Q., Wang, M., Sun, J., Gao, J. X., & Chen, J. (2017). Effect of trichoderma harzianum on maize rhizosphere microbiome and biocontrol of fusarium stalk rot. *Scientific Reports*, 7, 1–13. <https://doi.org/10.1038/s41598-017-01680-w>
- Schoebitz, M., López, M. D., & Roldán, A. (2013). Bioencapsulation of microbial inoculants for better soil-plant fertilization: A review. *Agron. Sustain. Dev.*, 33, 751–765. <https://doi.org/10.1007/s13593-013-0142-0>
- Seenivasagan, R., & Babalola, O. O. (2021). Utilization of microbial consortia as biofertilizers and biopesticides for the production of feasible agricultural product. *Biology (Basel)*, 10, 1111. <https://doi.org/10.3390/biology10111111>
- Su, Y. L., Fu, Z. Y., Zhang, J. Y., Wang, W. M., Wang, H., Wang, Y. C., & Zhang, Q. J. (2008). Microencapsulation of Radix salvia miltiorrhiza nanoparticles by spray-drying. *Powder Technology*, 184, 114–121. <https://doi.org/10.1016/j.powtec.2007.08.014>
- Uyanga, K. A., & Daoud, W. A. (2021). Green and sustainable carboxymethyl cellulose-chitosan composite hydrogels: Effect of crosslinker on microstructure. *Cellulose*, 28, 5493–5512. <https://doi.org/10.1007/s10570-021-03870-2>
- Vanderfleet, O. M., & Cranston, E. D. (2021). Production routes to tailor the performance of cellulose nanocrystals. *Nature Reviews Materials*, 6, 124–144. <https://doi.org/10.1038/s41578-020-00239-y>
- Vassilev, N., Vassileva, M., Martos, V., Garcia del Moral, L. F., Kowalska, J., Tytkowski, B., & Malusá, E. (2020). Formulation of microbial inoculants by encapsulation in natural polysaccharides: Focus on beneficial properties of carrier additives and derivatives. *Frontiers in Plant Science*, 11, 1–9. <https://doi.org/10.3389/fpls.2020.00270>
- Ye, L., Zhao, X., Bao, E., Li, J., Zou, Z., & Cao, K. (2020). Bio-organic fertilizer with reduced rates of chemical fertilization improves soil fertility and enhances tomato yield and quality. *Scientific Reports*, 10, 177. <https://doi.org/10.1038/s41598-019-56954-2>
- Zhang, F., Ge, H., Zhang, F., Guo, N., Wang, Y., Chen, L., Ji, X., & Li, C. (2016). Biocontrol potential of trichoderma harzianum isolate T-alo against sclerotinia sclerotiorum in soybean. *Plant Physiology and Biochemistry*, 100, 64–74. <https://doi.org/10.1016/j.plaphy.2015.12.017>